Process parameters for the high-scale production of alginate-encapsulated stem cells for storage and distribution throughout the cell therapy supply chain

Stephen Swioklo [a,1], Ping Ding [b,1], Andrzej W. Pacek [b], Che J. Connon [a,*]

[a] Institute of Genetic Medicine, Newcastle University, Newcastle Upon Tyne, UK
[b] School of Chemical Engineering, University of Birmingham, Birmingham, UK

ABSTRACT

With the ever-increasing clinical application of cell-based therapies, it is considered critical to develop systems that facilitate the storage and distribution of cell therapy products (CTPs) between sites of manufacture and the clinic. For such systems to be realized, it is essential that downstream bioprocessing strategies be established that are scalable, reproducible and do not influence the viability or function of the living biologic. To this end, we examined alginate-encapsulation as a method to heighten the preservation of human adipose-derived stem cells (hASCs) during hypothermic storage, and establish a scalable process for high-volume production. A drop-wise method for scalable alginate bead generation, using calcium as the cross-linker, was modified to enable the yield of up to 3500 gelled beads per minute. The effect of alginate concentration on the viscosity of non-gelled sodium alginate and the mechanical properties and internal structure of calcium-crosslinked alginate in response to different alginate and calcium concentrations were investigated. Mechanical strength was chiefly dependent on alginate concentration and 1.2% alginate cross-linked with 100 mM calcium chloride could withstand stress in the order of 35 kPa. Upon selection of appropriate parameters, we demonstrated the suitability of using this method for immobilizing human stem cells. Encapsulated hASCs demonstrated no loss in cell viability, and had a uniform distribution after high-volume production. Following storage, released cells were able to attach and recover a normal morphology upon return to culture conditions. Thus we present a scalable method for stem cell encapsulation and storage for application within the cell therapy supply chain.

1. Introduction

Advances in cell-based therapeutics have been considerable in recent times, with increasing numbers of clinical trials registered for the treatment of a vast array of disorders ranging from cardiovascular disease to cancer [1–3]. Many of these trials are in phase III of development and, accompanying this, is the Food and Drug Administration (FDA)- or European Medicines Agency (EMA)-approval of a number of cell therapy products (CTPs) as previously discussed [4].

One of the major hurdles faced for the clinical delivery of CTPs to the patient is in their upstream and downstream bioprocessing. In order to satisfy the number of cells required for cell based-therapies, typically being up to $1–2 \times 10^6$ cells/kg for mesenchymal stem cell (MSC)-based therapies [5], much effort has been spent in optimizing the expansion and reproducibility of cells for patient delivery [6]. Whilst it is fundamental to have in place rigorous platforms for upstream production of cell therapy products, it is also of utmost importance to develop scalable downstream bioprocessing strategies in order to meet clinical demand. Additionally, the final cell therapy product must be in a form that can be easily packaged, stored and distributed throughout the cell therapy supply chain.

Alginate, a natural polysaccharide derived from seaweed, has been used extensively as a hydrogel scaffold for cell delivery [7–9] due to its ease of gelation/de-gelation, biocompatibility, mass transfer properties, and its shielding effect facilitating the immunoisolation of encapsulated cells. As well as its use in scalable manufacturing for cell therapy applications [10], alginate has been

* Corresponding author at: Institute of Genetic Medicine, Faculty of Medicine, Newcastle University, International Centre for Life, Newcastle Upon Tyne, NE1 3BZ, UK.
E-mail addresses: Stephen.Swioklo@ncl.ac.uk (S. Swioklo), P.Ding@bham.ac.uk (P. Ding), A.W.Pacek@bham.ac.uk (A.W. Pacek), Che.Connon@ncl.ac.uk (C.J. Connon).
[1] These authors contributed equally to this manuscript.

demonstrated to be a useful matrix for the handling and storage of cells at hypothermic temperatures, whilst preserving cell viability and function [4,10–13].

The hypothermic storage of cells involves their maintenance, in a suspended state, at temperatures between 0 °C and 32 °C. Cells are then re-activated upon return to normothermic temperatures [14]. Due to the biological and technical issues associated with cryopreservation [15,16], the risk of thawing and wastage during transport, as well as the cost of infrastructure and equipment necessary for the storage and distribution of cryopreserved cells [17], there is much interest in the use of hypothermic preservation within the cell therapy supply chain [18,19]. The restricted, inflexible shelf lives associated with hypothermically stored CTPs can, however, still result in a high wastage of materials [20]. Therefore, methods that are able to improve the hypothermic preservation of cell viability and function, such as alginate-encapsulation, have a considerable potential.

In order to fulfill this potential, it is important to establish a downstream process for cell encapsulation that is scalable, reproducible and cost-effective. It is also imperative that the process does not affect cell viability and/or function. The gelation of alginate is most commonly performed through crosslinking polymers with divalent cations, such as calcium. This simple method of gelation allows the formation of alginate hydrogels of different shapes and dimensions, but most frequently alginate beads are produced. The method for bead generation can be performed by either external or internal gelation. The former involves the diffusion of an exogenous source of cations for alginate crosslinking, whereas internal gelation requires an insoluble source of crosslinking ions within the alginate. For bead generation, the latter of these is carried out through the suspension of alginate solution in oil phase followed by the release of crosslinking ions, most typically by lowering pH through the addition of organic acids [21–23]. However, internal gelation is also associated with (1) typically long gelling times in the range of several hours [24] and (2) the necessity to lower the pH value, which may influence the viability of immobilized cells [22]. The advantages of externally gelled hydrogels are; (1) short gelling times (in the range of seconds to minutes), and (2) no potential contamination of stem cells by oil and the associated difficulties in separating the gelled beads from the oil phase are eliminated. Therefore, external gelation using an alginate-calcium two phase aqueous system has important advantages for stem cell encapsulation, specifically for large-scale applications.

Human adipose-derived stem cells (hASCs), a source of MSCs from subcutaneous fat, have a considerable clinical interest with over 130 clinical trials being registered for their use between February 2007 and April 2015 (as listed on clinicaltrials.gov). Using these cells, we explored a modified drop-wise bead generation as a method for scalable hASC encapsulation. We assessed the mechanical properties of non-gelled sodium alginate solubilized in PBS and subsequently gelled calcium-crosslinked alginate. We then examined the mechanical strength of calcium alginate beads in response to different alginate and calcium concentrations. Following the selection of appropriate process parameters, we demonstrated that encapsulating hASCs in alginate using this method did not impact cell viability, and facilitated an even distribution of live and dead cells throughout alginate beads. Finally, we examined hASC morphology and capacity to attach (to tissue culture plastic) following return to normal cell culture conditions after periods of cell storage, demonstrating that this is a suitable method to maintain the cytoprotective properties of alginate whilst exploiting a highly scalable downstream platform.

2. Materials and methods

2.1. Rheological assessment of sodium alginate viscosity

The flow curves of 0.6–2.4% (w/v) sodium alginate (Aldrich brand #W201502, Sigma Aldrich, UK) in PBS (Oxoid brand, Fisher Scientific, UK) was measured using a Bohlin rheometer with 4 cm cone-and-plate geometry (Malvern instrument, UK).

2.2. Preparation of alginate beads

The gelation of alginate beads was performed in a baffled jacketed stirred vessel of 75 mm diameter fitted with a 42 mm Rushton turbine impeller. A volume of 250 mL, 100 mM $CaCl_2$ was charged into the vessel kept at 20 °C and stirred at 130 rpm to uniformly suspend gelling alginate beads. A custom-made extrusion head composed of 9 needles (internal diameter 0.6 mm) was placed 10–15 mm above the calcium solution. Alginate solution was extruded at a flow rate of 22 mL/min using a peristaltic pump and the formed beads were subsequently stirred and allowed to gel for 10 min. The images of gelled beads were recorded *in-situ* using a stereo-microscope fitted with a video camera and bead size distribution and mean diameter were measured by image analysis.

2.3. Measurement of mechanical properties of gelled beads

The mechanical properties of beads manufactured with different concentrations of alginate and calcium chloride ($CaCl_2$) were measured using a Static Materials Testing Machine (Zwick/Roell, 2030). Gelled beads (~2.8 mm diameter) were compressed by a stainless steel probe connected to a force transducer and a computer allowing precise control of the probe position and speed of compression. During the test the compressive force and the displacement were continuously recorded. The zero displacement was defined when the probe touched the surface of the beads (zero force). Deformation was defined as the displacement divided by the bead's diameter. The stress was defined as the force divided by the area of the initial cross section of the bead. For every experimental condition, 10 beads were measured and the average values of displacement and force were calculated.

2.4. Structural characterization of gelled alginate beads by ESEM

The internal structure of gelled beads was examined by an Environmental Scanning Electron Microscope (ESEM, Philips XL30). Gelled beads withdrawn from the calcium bath were washed three times in double distilled water followed by washing for 15 min in each of the following ethanol solutions: 50% (v/v), 70% (v/v), 90% (v/v) and 100%. Then, the beads were dehydrated using critical point drying, fractured to expose an internal structure, placed on aluminum stubs, and coated with gold before examination using ESEM.

2.5. hASC culture

hASCs obtained from the subcutaneous fat of three healthy donors (Invitrogen, UK), were used for experiments. Cells were isolated from both male and female subjects (aged 45–63 years) and purity was determined by the manufacturer as cells being ≥95% positive for CD29, CD44, CD73, CD90, CD105, and CD166 and ≤2% positive for CD14, CD31 and CD45 surface antigen expression. Following recovery from cryostorage, cells were seeded at 800 cells/cm² and maintained in reduced-serum (RS) growth media [MesenPRO™ RS medium containing 2 mM GlutaMAX™ and 1% (v/v) antibiotic-antimycotic (all from Life Technologies, UK)] in a humidified incubator at 37 °C and 5% CO_2 with medium changes
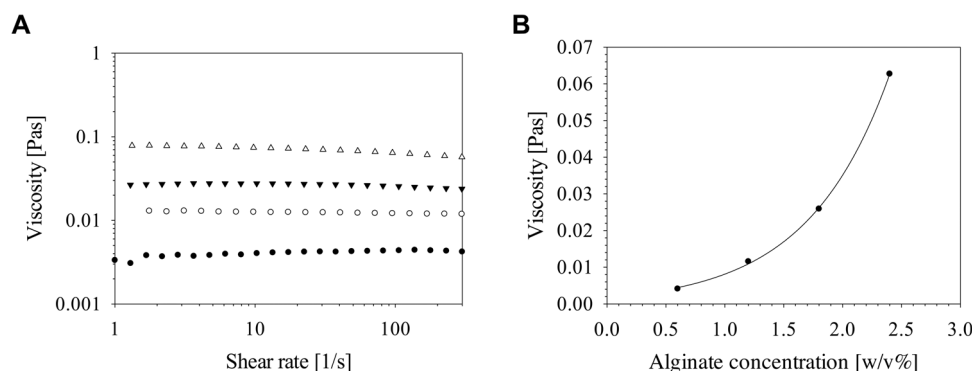
A

B

Fig. 1. Rheology of sodium alginate solutions. (A) flow curves at different alginate concentrations: (●) 0.6% (w/v), (○) 1.2% (w/v), (▼) 1.8% (w/v), (△) 2.4% (w/v); (B) viscosity as a function of alginate concentration.

every 3–4 days until approximately 80% confluence was reached. Cells were harvested using TrypLE[TM] Express enzyme (Life Technologies, UK).

2.6. Encapsulation of hASCs

A sample of harvested cells was incubated with 0.2% Trypan Blue (Invitrogen, UK) for 3 min before counting viable (unstained) and dead (stained) cells using a Neubauer haemocytometer. A 30 mL suspension of 1×10^6 viable cells/mL in growth media was then mixed with 30 mL 2.4% (w/v) sodium alginate in PBS. Alginate beads containing cells were then extruded as per materials and methods Section 2.2. Following gelation, beads were washed briefly in PBS before storing approximately 5 mL of gelled beads in tightly sealed 15 mL centrifuge tubes containing 10 mL growth medium to occupy the full volume of the tube.

2.7. Determination of percentage cell viability

Cells were assessed for percentage cell viability before, immediately after, and 24 h after encapsulation. For the assessment of encapsulated samples, cells were first released by dissolving calcium alginate using 100 mM trisodium citrate (Sigma, UK) for 5 min at room temperature. Trisodium citrate was diluted using PBS before separating cells by centrifugation. Released cells were resuspended in growth medium and incubated with 0.2% Trypan Blue (Invitrogen, UK) for 3 min before counting viable (unstained) and dead (stained) cells using a Neubauer haemocytometer. Percentage viability was calculated as the number of viable cells divided by the total number of cells, multiplied by 100.

2.8. Determination of live cell distribution throughout alginate beads

48 h after cell encapsulation, phase-contrast images were captured using an Axiovert 200 M inverted microscope (Zeiss, UK). Live and dead cell distribution was assessed following incubation with 1 μM Calcein-AM (eBioscience, UK) and 2 μM ethidium homodimer-1 (Sigma Aldrich, UK) for 30 min at 37 °C before assessing cell distribution using an A1R confocal microscope (Nikon, UK). Further examination of cell distribution was achieved following incubation with 0.2 μM CellTag 700 and capturing images of beads using an Odyssey CLx Infrared imager (both from LI-COR Biosciences, UK).

2.9. Assessment of cell attachment following storage in alginate beads

Cells were assessed for their ability to attach to tissue culture plastic under normal cell culture conditions both 1 day and 7 days after encapsulation (and release) and compared to non-encapsulated cells treated in the same manner. For the longer storage time, cells were stored at 15 °C in a cooled incubator with atmospheric O_2 and CO_2 in tightly sealed 15 mL centrifuge tubes containing growth medium to occupy the full volume of the tube (as per materials and methods Section 2.6). Non-encapsulated cells were simply suspended in the same volume of growth medium and stored in tightly sealed tubes. Following release from storage, calcium alginate beads were dissolved and cells separated as per materials and methods Section 2.7. Cells were then dissociated using TrypLE Express Enzyme (Invitrogen, UK) for 5 min at room temperature. This was necessary due to aggregation of control (non-encapsulated) samples during the storage period. Following dissociation, an equal volume of growth medium to TrypLE Express was added before cells were counted and plated at 5000 cells/cm² in 24-well plates containing growth medium. After 24 h at 37 °C, 5% CO_2 in a humidified incubator, images were captured of attached cells.

2.10. Statistical analysis

Statistical analysis for percentage viability measurements was carried out using GraphPad Prism (v6.00). Data are expressed as means of values from three separate donors ± standard deviation (SD). Statistical comparisons were made using one-way repeated measures Analysis of Variance (ANOVA) with Bonferroni post hoc tests.

3. Results and discussion

3.1. Characterization of sodium alginate solutions in PBS

Prior to bead generation, the flow curves of alginate solutions in PBS were measured over the range of alginate concentrations. Up to alginate concentrations of 2.4% (w/v), solutions were practically Newtonian (Fig. 1A) with viscosity increasing exponentially with alginate concentrations (Fig. 1B). Based on the calculated intrinsic viscosity using the data in Fig. 1, the molecular weight of the alginate was estimated as 83 kDa ± 5.45 kDa [25–27]. The critical concentration, where the gel encompasses the whole volume of the solution, was estimated as 0.37% (w/v) [28]. In the experiments discussed here the alginate concentration was in the range from
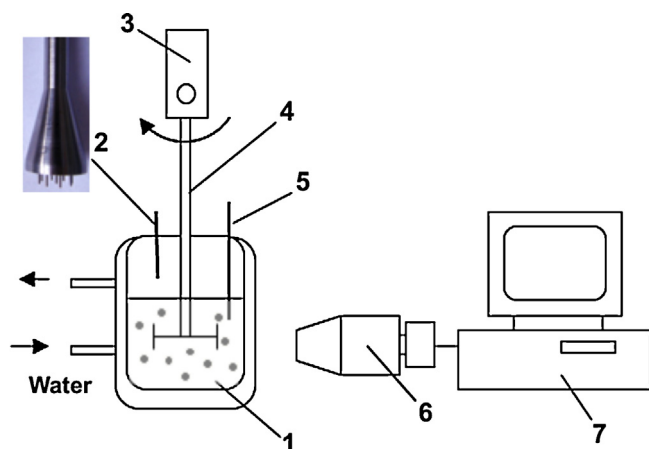
Fig. 2. Schematic of experimental rig used for alginate bead generation. 1- jacketed stirred vessel, 2- home made extrusion head, 3-stirrer, 4- Rushton turbine, 5- strobe light, 6- microscope combined with video camera, 7- image acquisition system.

0.6 to 2.4 g/ml, which is well above the critical concentration i.e. the minimum concentration for gelation.

3.2. Drop-wise method for bead generation

Of the methods established for the generation of alginate beads, the drop-wise method is the most established and technically least challenging. In order to increase the production rate of alginate beads, the standard extrusion method was modified using a custom-made extrusion head with multiple needles. This was designed in such a way to prevent coalescence of alginate on the surface of the head whilst being easily cleaned and sterilized (see Fig. 2). Through using this approach, it was possible to yield an increased production rate of calcium alginate beads, approximately 3500 beads/min of 2.8 ± 0.15 mm diameter and very narrow size distribution. Thus, this method represented a highly scalable approach for the production of large numbers of alginate beads for cell immobilization. Prior to cell encapsulation, the effect of alginate and calcium concentrations on mechanical and structural properties of beads generated by this method was investigated.

3.3. Mechanical properties of calcium alginate beads

The mechanical properties of the gelled beads are summarized in Figs. 3 and 4. Fig. 3A shows the stress as a function of deformation and it is clear that at around 60% deformation, gelled beads fracture (point A in Fig. 3A). Fig. 3B shows typical results of the press-release experiments with the characteristic hysteresis loop where at zero stress, beads are significantly deformed. This clearly

indicates that gelled alginate beads are elasto-plastic. This was also confirmed by press-hold tests where, at constant deformation, the compressive force gradually decreases with the relaxation time. Elasto-plastic behavior might be explained by the high porosity of gelled beads and it is consistent with the high permeability of alginate gels [29,30] and ESEM measurements discussed below. High porosity allows the inflow of oxygen and nutrients to and the outflow of therapeutic factors, metabolites and waste products from gelled beads confirming the suitability of alginate beads for preservation/encapsulation of stem cells.

The mechanical strength of the beads increased with alginate concentrations (Fig. 4A). This could be explained by the fact that as the alginate concentrations increased, the gel network became denser and stronger, leading to the increase in overall mechanical strength. However, calcium concentrations seem to have little effect on the gel structure and mechanical strength as shown in Fig. 4B. This is also consistent with the results of ESEM measurement discussed below.

3.4. Morphology of gelled alginate beads

The effect of alginate concentrations on the morphology of gelled beads is shown in Fig. 5. As the alginate concentration was increased the pores inside beads became smaller. This is consistent with the author's previous results [13] and also with the mechanical strength measurements discussed above showing that the strength of beads increased with the alginate concentrations. Fig. 5 also shows that the pore size is practically independent of calcium concentrations range from 0.07 to 0.15 M. This is also consistent with the mechanical measurement where the strength of beads is practically independent of the calcium concentrations.

It is worth noting that at high calcium concentrations, specifically at 0.15 M, calcium crystals were observed inside pores implying calcium salt precipitation during drying.

3.5. Selection of process conditions for stem cell encapsulation

For cell encapsulation, 1.2% (w/v) alginate and 0.1 M calcium chloride concentrations were selected. These concentrations had been previously demonstrated to be suitable in alginate-based systems that convey cytoprotection during hypothermic storage [4,11,13] and were deemed appropriate following mechanical and structural characterization. Whilst we demonstrated that increasing the concentration of sodium alginate did result in an increased mechanical strength, which may be favorable for durability of the final product, the decreased pore size at higher concentrations may effect the mass transfer properties of the gel which could be critical for cell survival. Additionally, the higher viscosity of more concentrated alginate solutions may have compromised the even
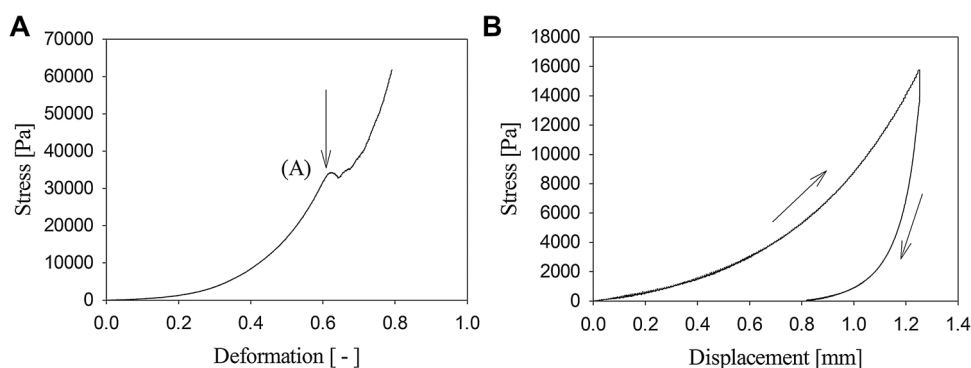

Fig. 3. Mechanical properties of calcium alginate beads. (A) stress as a function of deformation, (B) example of press-release curve in 1.2% (w/v) alginate gelled in and 100 mM CaCl$_2$.
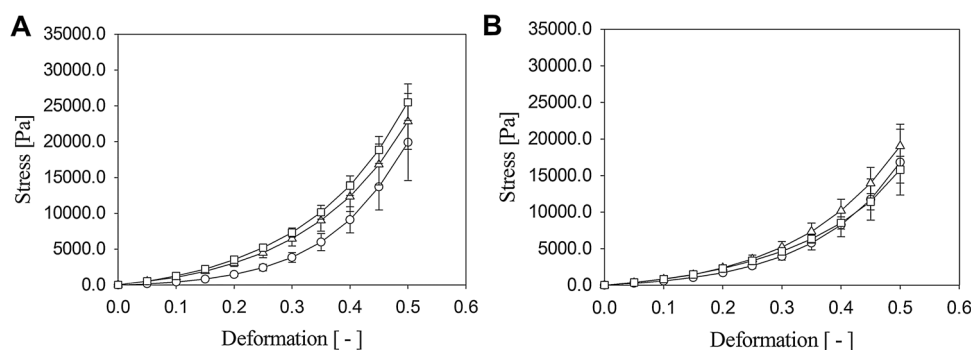
Fig. 4. Mechanical strength of alginate beads. (A) effect of alginate concentration at constant calcium concentration of 0.1 M CaCl$_2$: (○) 1.2% (w/v) alginate, (△) 1.8% (w/v) alginate, (□) 2.4% (w/v); (B) effect of calcium concentration at constant alginate concentration 1.2% (w/v) alginate: (○) 0.07 M CaCl$_2$, (△) 0.1 M CaCl$_2$, (□) 0.15 M CaCl$_2$.
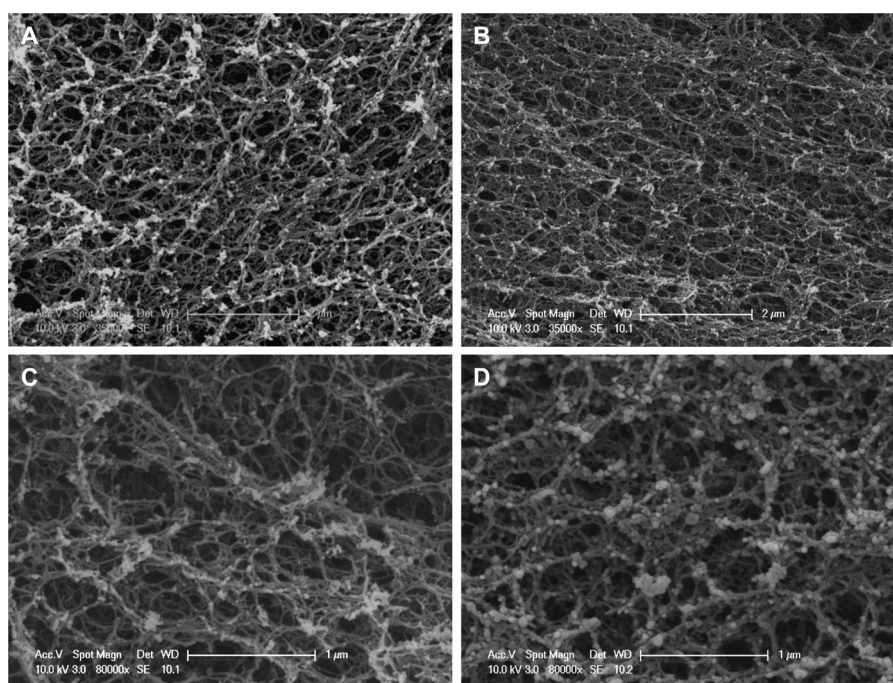

Fig. 5. Effect of alginate and calcium concentrations on the structure of gelled beads. (A) 1.2% (w/v) alginate, 0.1 M CaCl$_2$; (B) 2.4% (w/v) alginate, 0.1 M CaCl$_2$; (C) 1.2% (w/v) alginate 0.07 M CaCl$_2$; (D) 1.2% (w/v) alginate, 0.15 M CaCl$_2$.

distribution of cells throughout the hydrogel, and increased the shear stress inflicted on cells during distribution and extrusion, as well as increasing the possibility of blockages forming in the extrusion system (the latter point was indeed observed on several occasions with 1.8%–2.4% (w/v) alginate concentrations). The effect of calcium chloride concentration on the mechanical properties of gelled alginate was negligible in the range tested, whilst higher concentrations resulted in salt formation. We therefore selected 0.1 M calcium chloride as a gelling solution that allowed reproducible bead formation and no evidence of calcium salts within the matrix. Using these conditions, the modified drop-wise method for bead generation was employed to encapsulate hASCs.

3.6. The effect of processing on cell viability

Due to the possible exposure of cells to shear stress during extrusion and gelation, it was important to determine whether the process had a negative impact on cell viability. This was performed both directly after processing, and 24 h after processing in order to take into account any delayed activation of cellular stress pathways. An even distribution of hASCs throughout gelling alginate
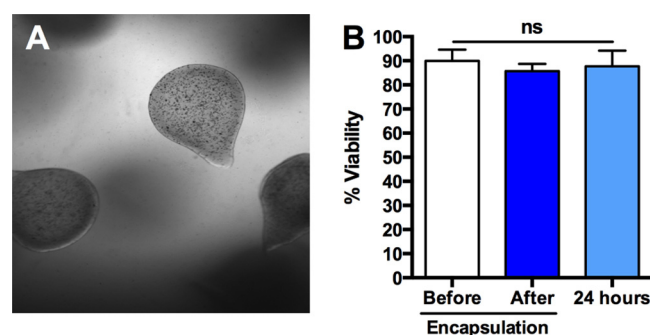

Fig. 6. The effect of processing on cell viability. Images of cells encapsulated in alginate were monitored during gelation (A) and the percentage viability of cells was measured before, immediately after, and 24 h after encapsulation (B). Values are expressed as means ± SD from 3 separate donors.

beads was observed during encapsulation (Fig. 6A) and encapsulated cells exhibited no significant decrease in percentage viability (Fig. 6B) with levels of 90 ± 5%, 86 ± 3% and 88 ± 7% before, after and 24 h after processing respectively.
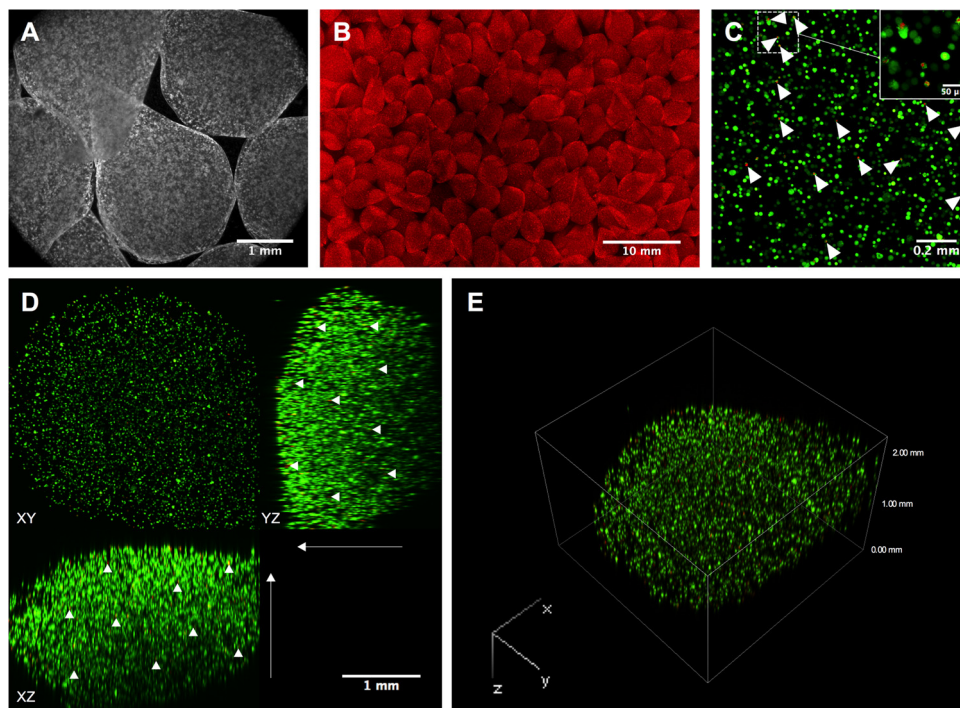
Fig. 7. The spatial distribution of cells through alginate beads. 48 h after encapsulation, hASCs in beads were examined by phase microscopy (A), infrared imaging (B) and confocal microscopy (C–E). (C–E) hASCs were stained with calcein-AM (live indicator; green) and ethidium homodimer-1 (dead indicator: red) and maximal projection (C), orthogonal projection (D) and 3D projection (E) images were captured. Arrowheads indicate the position of dead cells. (For interpretation of the references to colour in this figure legend, the reader is referred to the web version of this article.)
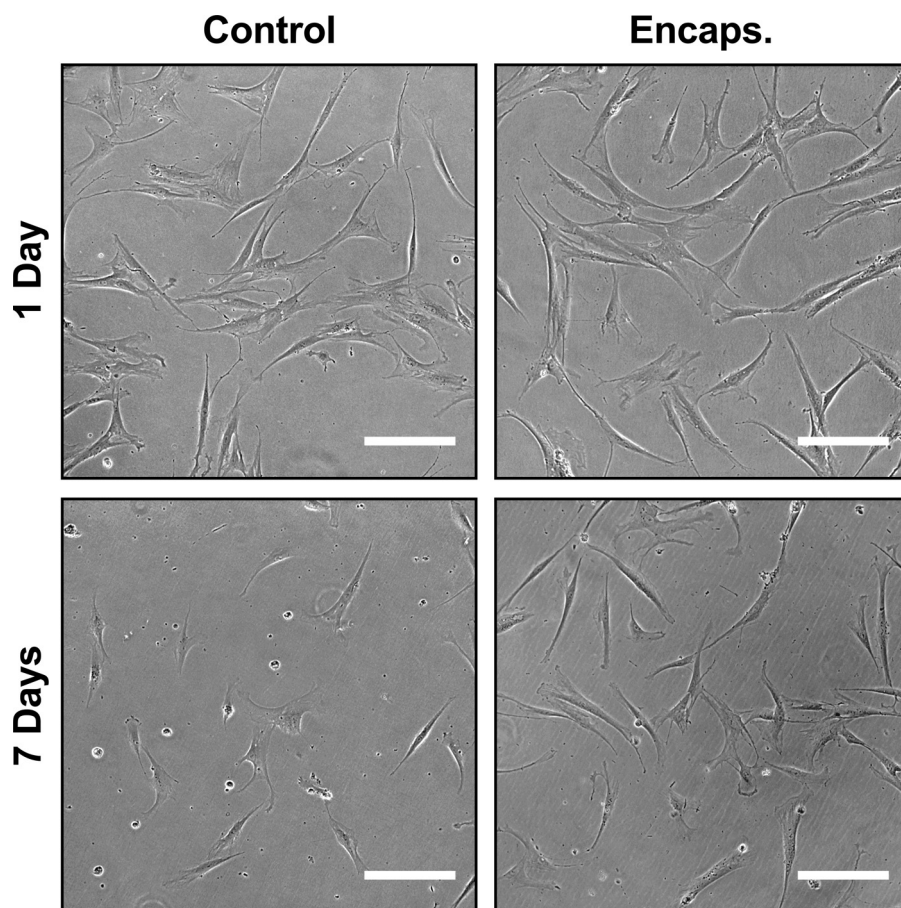

Fig. 8. Morphology and attachment of encapsulated ASCs following storage. hASCs were stored for either 1 day or 7 days before plating at 5000 cells/cm^2 and returning to normal tissue culture conditions. Scale bars = 200 μm.

With the method and parameters selected for cell encapsulation, it was fundamental that we determined that there was no adverse effect on cell viability owing to shear stress as has been reported in different alginate systems [31]. Using 1.2% (w/v) alginate, cells could be dispersed easily and quickly within the matrix before extrusion through multiple needles and gelation by ionic crosslinking. Using this simple drop-wise method, we were able to rapidly generate large numbers of beads without affecting the health of cell populations.

3.7. Viable and dead cell distribution throughout alginate beads

In order to further explore the spatial distribution of cells following encapsulation, as well as their viability, we employed a number of imaging techniques 48 h after bead generation. It is of great importance to maintain consistency in terms of cell number and uniformity during production, and this must be sustained throughout the whole production process.

Beads exhibited a spherical appearance with a slight tail (Fig. 7A), an appearance maintained following the production of a large number of beads (Fig. 7B). Importantly, cell distribution was uniform as demonstrated by infrared imaging of encapsulated cells, clearly depicting the shape of the beads with greater intensity at points of overlap (Fig. 7B). Confocal imaging of live/dead-stained encapsulated cells supported the high viability demonstrated at earlier time points, with cells exhibiting a good distribution from projected Z-stacks (Fig. 7C) and few dead cells (indicated by arrowheads). This was also apparent in orthogonal views of YZ and XZ planes (Fig. 7D) where both live and dead cells were distributed throughout the depth of the bead (dead cells indicated with arrowheads). The same cellular dispersal was represented by volume projection (Fig. 7E). The even distribution of dead cells, accompanied by the absent loss of viability described earlier, confirms that cell death is not being induced by the potential external stresses that cells are exposed to during processing.

3.8. Attachment and morphology of hASCs following release from storage

In addition to the effect of processing on cell viability, it was also essential to examine cellular function after a period of rewarming. The deterioration of cell viability and function within 24 h of return to normothermic conditions has been well described following cryopreservation [32] and hypothermic storage [33,34], associated with the delayed activation of apoptotic and necrotic pathways. It was also pertinent because bone marrow-derived MSCs have been reported to have attenuated attachment following hypothermic storage [35]. We therefore examined the attachment of hASCs upon return to normal tissue culture conditions for 24 h following hypothermic storage for 1 or 7 days. hASCs seeded 1 day after encapsulation exhibited a normal spindle shaped fibroblast-like morphology after 24 h in culture, demonstrating a good capacity for attachment (Fig. 8). No obvious differences were observed between encapsulated hASCs and non-encapsulated (control) samples stored in the same manner. After 7 days in storage however, alginate-encapsulation was demonstrated to preserve attachment (Fig. 8). Whilst encapsulated cells exhibited a reasonable level of attachment, albeit at a slightly lower level compared to 1 day, control samples demonstrated a considerable decrease in the number of attached cells, with a greater evidence of rounded, dead cells. The capacity for alginate-encapsulation to preserve the capacity for cells to attach following rewarming supports previous work conducted in our lab [4]. In this previous study, the hypothermic storage of non-encapsulated hASCs at 15 °C resulted in a significant decrease in the number of cells attaching to tissue culture plastic after return to normal tissue culture conditions. The encapsulation of cells in 1.2% calcium alginate discs prevented this decrease in attachment.

These results further support the suitability of this processing approach in maintaining the cytoprotective effects of alginate-encapsulation for hypothermic storage described previously [4,10–13].

4. Conclusions

Determining a scalable downstream processing platform that has no effect on cell viability is paramount to a successful cell-storage system. In this study, we have built on previous work demonstrating the cytoprotective effects of alginate encapsulation [4,11–13], and explored a suitable scalable method for the production of alginate-encapsulated stem cells for storage and distribution throughout the cell therapy supply chain. Alginate represents a versatile material with demonstrable cytoprotective effects and simple scalability in production, thus exhibiting considerable potential in the cell therapy industry.

References

[1] L. Foley, M. Whitaker, Concise review: cell therapies: the route to widespread adoption, Stem Cells Transl. Med. 1 (2012) 438–447.
[2] M.D. Li, H. Atkins, T. Bubela, The global landscape of stem cell clinical trials, Regen. Med. 9 (2014) 27–39.
[3] B.A. Syed, J.B. Evans, Stem cell therapy market, Nat. Rev. Drug Discov. 12 (2013) 185–186.
[4] S. Swioklo, A. Constantinescu, C.J. Connon, Alginate-encapsulation for the improved hypothermic preservation of human adipose-derived stem cells, Stem Cell Transl. Med. 5 (2016) 339–349.
[5] C. Ikebe, K. Suzuki, Mesenchymal stem cells for regenerative therapy: optimization of cell preparation protocols, Biomed Res. Int. (2014) 951512.
[6] T.G. Fernandes, C.A.V. Rodrigues, M.M. Diogo, J.M.S. Cabral, Stem cell bioprocessing for regenerative medicine, J. Chem. Technol. Biotechnol. 89 (2014) 34–47.
[7] M. Balyura, E. Gelfgat, M. Ehrhart-Bornstein, B. Ludwig, Z. Gendler, U. Barkai, B. Zimerman, A. Rotem, N.L. Block, A.V. Schally, S.R. Bornstein, Transplantation of bovine adrenocortical cells encapsulated in alginate, Proc. Natl. Acad. Sci. U. S. A. 112 (2015) 2527–2532.
[8] C. Ceccaldi, S.G. Fullana, C. Alfarano, O. Lairez, D. Calise, D. Cussac, A. Parini, B. Sallerin, Alginate scaffolds for mesenchymal stem cell cardiac therapy: influence of alginate composition, Cell Transplant. 21 (2012) 1969–1984.
[9] E.J. Wright, K.A. Farrell, N. Malik, M. Kassem, A.L. Lewis, C. Wallrapp, C.M. Holt, Encapsulated glucagon-like peptide-1-producing mesenchymal stem cells have a beneficial effect on failing pig hearts, Stem Cells Transl. Med. 1 (2012) 759–769.
[10] E. Erro, J. Bundy, I. Massie, S.-A. Chalmers, A. Gautier, S. Gerontas, M. Hoare, P. Sharratt, S. Choudhury, M. Lubowiecki, I. Llewellyn, C. Legallais, B. Fuller, H. Hodgson, C. Selden, Bioengineering the liver: scale-up and cool chain delivery of the liver cell biomass for clinical targeting in a bioartificial liver support system, Biores. Open Access 2 (2013) 1–11.
[11] B. Chen, B. Wright, R. Sahoo, C.J. Connon, A novel alternative to cryopreservation for the short-term storage of stem cells for use in cell therapy using alginate encapsulation, Tissue Eng. Part C-Methods 19 (2013) 568–576.
[12] S. Mahler, M. Desille, B. Fremond, C. Chesne, A. Guillouzo, J.P. Campion, B. Clement, Hypothermic storage and cryopreservation of hepatocytes: the protective effect of alginate gel against cell damages, Cell Transplant. 12 (2003) 579–592.
[13] B. Wright, R.A. Cave, J.P. Cook, V.V. Khutoryanskiy, S.L. Mi, B. Chen, M. Leyland, C.J. Connon, Enhanced viability of corneal epithelial cells for efficient transport/storage using a structurally modified calcium alginate hydrogel, Regen. Med. 7 (2012) 295–307.
[14] J. Baust, J. Baust, Concepts in biopreservation, Adv. Biopreserv. (2007) 1–14.
[15] R. Pal, M. Hanwate, S.M. Totey, Effect of holding time, temperature and different parenteral solutions on viability and functionality of adult bone

marrow-derived mesenchymal stem cells before transplantation, J. Tissue Eng. Regen. Med. 2 (2008) 436–444.

[16] S. Thirumala, W.S. Goebel, E.J. Woods, Manufacturing and banking of mesenchymal stem cells, Expert Opin. Biol. Ther. 13 (2013) 673–691.

[17] P. Loi, D. Iuso, M. Czernik, F. Zacchini, G. Ptak, Towards storage of cells and gametes in dry form, Trends Biotechnol. 31 (2013) 688–695.

[18] P. Hourd, P. Ginty, A. Chandra, D.J. Williams, Manufacturing models permitting roll out/scale out of clinically led autologous cell therapies: regulatory and scientific challenges for comparability, Cytotherapy 16 (2014) 1033–1047.

[19] D.H. Pamphilon, E. Selogie, Z.M. Szczepiorkowski, Transportation of cellular therapy products: report of a survey by the cellular therapies team of the Biomedical Excellence for Safer Transfusion (BEST) collaborative, Vox Sang. 99 (2010) 168–173.

[20] C.A. Hernon, R.A. Dawson, E. Freedlander, R. Short, D.B. Haddow, M. Brotherston, S. MacNeil, Clinical experience using cultured epithelial autografts leads to an alternative methodology for transferring skin cells from the laboratory to the patient, Regen. Med. 1 (2006) 809–821.

[21] K.I. Draget, K. Ostgaard, O. Smidsrod, Homogeneous alginate gels – a technical approach, Carbohydr. Polym. 14 (1990) 159–178.

[22] C.A. Hoesli, K. Raghuram, R.L.J. Kiang, D. Mocinecova, X.K. Hu, J.D. Johnson, I. Lacik, T.J. Kieffer, J.M. Piret, Pancreatic cell immobilization in alginate beads produced by emulsion and internal gelation, Biotechnol. Bioeng. 108 (2011) 424–434.

[23] E. Papajova, M. Bujdos, D. Chorvat, M. Stach, I. Lacik, Method for preparation of planar alginate hydrogels by external gelling using an aerosol of gelling solution, Carbohydr. Polym. 90 (2012) 472–482.

[24] C.K. Kuo, P.X. Ma, Maintaining dimensions and mechanical properties of ionically crosslinked alginate hydrogel scaffolds in vitro, J. Biomed. Mater. Res. A 84A (2008) 899–907.

[25] A. Martinsen, G. Skjakbraek, O. Smidsrod, F. Zanetti, S. Paoletti, Comparison of different methods for determination of molecular-weight and molecular-weight distribution of alginates, Carbohydr. Polym. 15 (1991) 171–193.

[26] O. Smidsrod, A. Haug, A light scattering study of alginate, Acta Chem. Scand. 22 (1968) 797–810.

[27] B.T. Stokke, K.I. Draget, O. Smidsrod, Y. Yuguchi, H. Urakawa, K. Kajiwara, Small-angle X-ray scattering and rheological characterization of alginate gels 1. Ca-alginate gels, Macromolecules 33 (2000) 1853–1863.

[28] A. Mikkelsen, A. Elgsaeter, Density distribution of calcium-induced alginate gels – a numerical study, Biopolymers 36 (1995) 17–41.

[29] M. Brissova, I. Lacik, A.C. Powers, A.V. Anilkumar, T. Wang, Control and measurement of permeability for design of microcapsule cell delivery system, J. Biomed. Mater. Res. 39 (1998) 61–70.

[30] E. Favre, M. Leonard, A. Laurent, E. Dellacherie, Diffusion of polyethyleneglycols in calcium alginate hydrogels, Colloid Surface A 194 (2001) 197–206.

[31] H.J. Kong, M.K. Smith, D.J. Mooney, Designing alginate hydrogels to maintain viability of immobilized cells, Biomaterials 24 (2003) 4023–4029.

[32] A. Bissoyi, B. Nayak, K. Pramanik, S.K. Sarangi, Targeting cryopreservation-induced cell death: a review, Biopreserv. Biobanking 12 (2014) 23–34.

[33] W.L. Corwin, J.M. Baust, R.G. Vanbuskirk, J.G. Baust, In vitro assessment of apoptosis and necrosis following cold storage in a human airway cell model, Biopreserv. Biobanking 7 (2009) 19–27.

[34] W.L. Corwin, J.M. Baust, J.G. Baust, R.G. Van Buskirk, Characterization and modulation of human mesenchymal stem cell stress pathway response following hypothermic storage, Cryobiology 68 (2014) 215–226.

[35] E. Veronesi, A. Murgia, A. Caselli, G. Grisendi, M.S. Piccinno, V. Rasini, R. Giordano, T. Montemurro, P. Bourin, L. Sensebe, M.T. Rojewski, H. Schrezenmeier, P. Layrolle, M.P. Ginebra, C.B. Panaitescu, E. Gomez-Barrena, F. Catani, P. Paolucci, J.S. Burns, M. Dominici, Transportation conditions for prompt use of ex vivo expanded and freshly harvested clinical-grade bone marrow mesenchymal stromal/stem cells for bone regeneration, Tissue Eng. Part C-Methods 20 (2014) 239–251.